Supporting Information for

Beyond 22% Power Conversion Efficiency in Type-II $MoSi_2As_4/MoGe_2N_4$ Photovoltaic vdW Heterostructure

Jing-yi Zhang[a,b], Xiao-bin Wu[*a,b] and Jun-jie Shi[c]

[a] *Opto-electronic Center, Institute of Microelectronics of the Chinese Academy of Sciences, Beijing 100029, China.*

[b] *School of Integrated Circuits, University of Chinese Academy of Sciences, Beijing 100049, China.*

[c] *State Key Laboratory for Artificial Microstructures and Mesoscopic Physics, School of Physics, Peking University Yangtze Delta Institute of Optoelectronics, Peking University, Beijing 100871, China.*

E-mail: wuxiaobin@ime.ac.cn

Convergence testing of the *k* mesh and cut-off energy

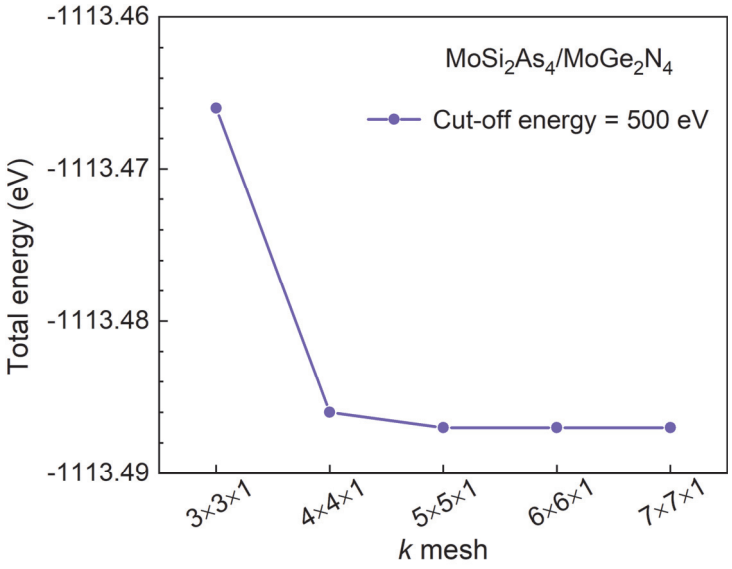

Fig. S1 Convergence assessment of the *k*-point mesh on the total energy for the $MoSi_2As_4/MoGe_2N_4$ vdW heterostructure utilizing a cut-off energy of 500 eV. The total energy variation ranges from -1113.487 to -1113.466 eV. Upon increasing the *k*-point density from a 4×4×1 grid to more refined meshes, the total energy change was found to be less than 1 meV per atom, indicating that the results for energy had converged to the required accuracy. Therefore, a *k*-point mesh of 5×5×1 was selected for subsequent computational analyses.

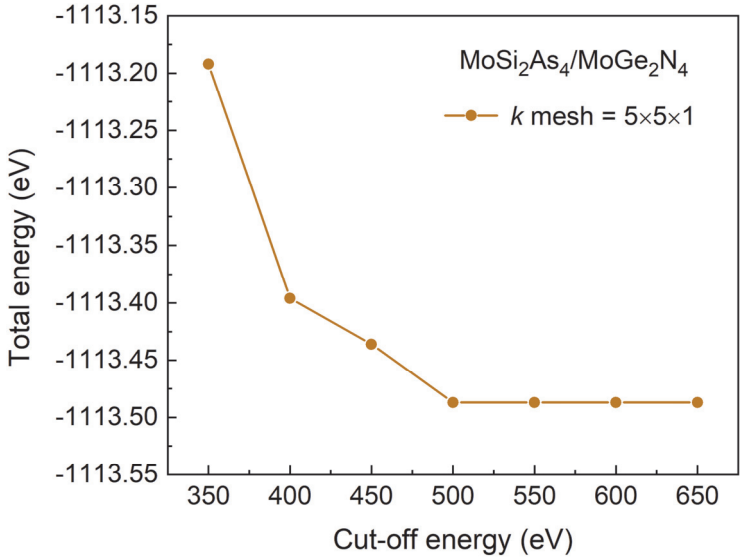

Fig. S2 Convergence assessment of the cut-off energy on the total energy for the $MoSi_2As_4/MoGe_2N_4$ vdW heterostructure, employing a *k*-point mesh of 5×5×1. The results indicate that beyond a cut-off energy of 450 eV, the total energy difference is negligible (0.051 eV), and the average total energy change per atom is less than 0.5 meV. Consequently, a cut-off energy of 500 eV was selected for the present calculations to ensure numerical accuracy.

Table S1. Lattice constants *a*/*b*, total energy E_{TOT}, interlayer spacing *d*, PBE band gap E_g and formation energy E_f of eight configurations for $MoSi_2As_4/MoGe_2N_4$ vdW heterostructure

Configuration	*a*/*b* (Å)	E_{TOT} (eV)	*d* (Å)	E_g (eV)	E_f (meV/atom)
C1	10.832	-1113.465	3.423	0.302	-13.120
C2	10.779	-1113.469	3.411	0.305	-13.146
C3	10.875	-1113.463	3.405	0.300	-13.107
C4	10.828	-1113.461	3.412	0.302	-13.094
C5	10.782	-1113.467	3.406	0.299	-13.133
C6	10.783	-1113.471	3.401	0.302	-13.159
C7	10.833	-1113.473	3.391	0.300	-13.172
C8	10.831	-1113.471	3.392	0.299	-13.159

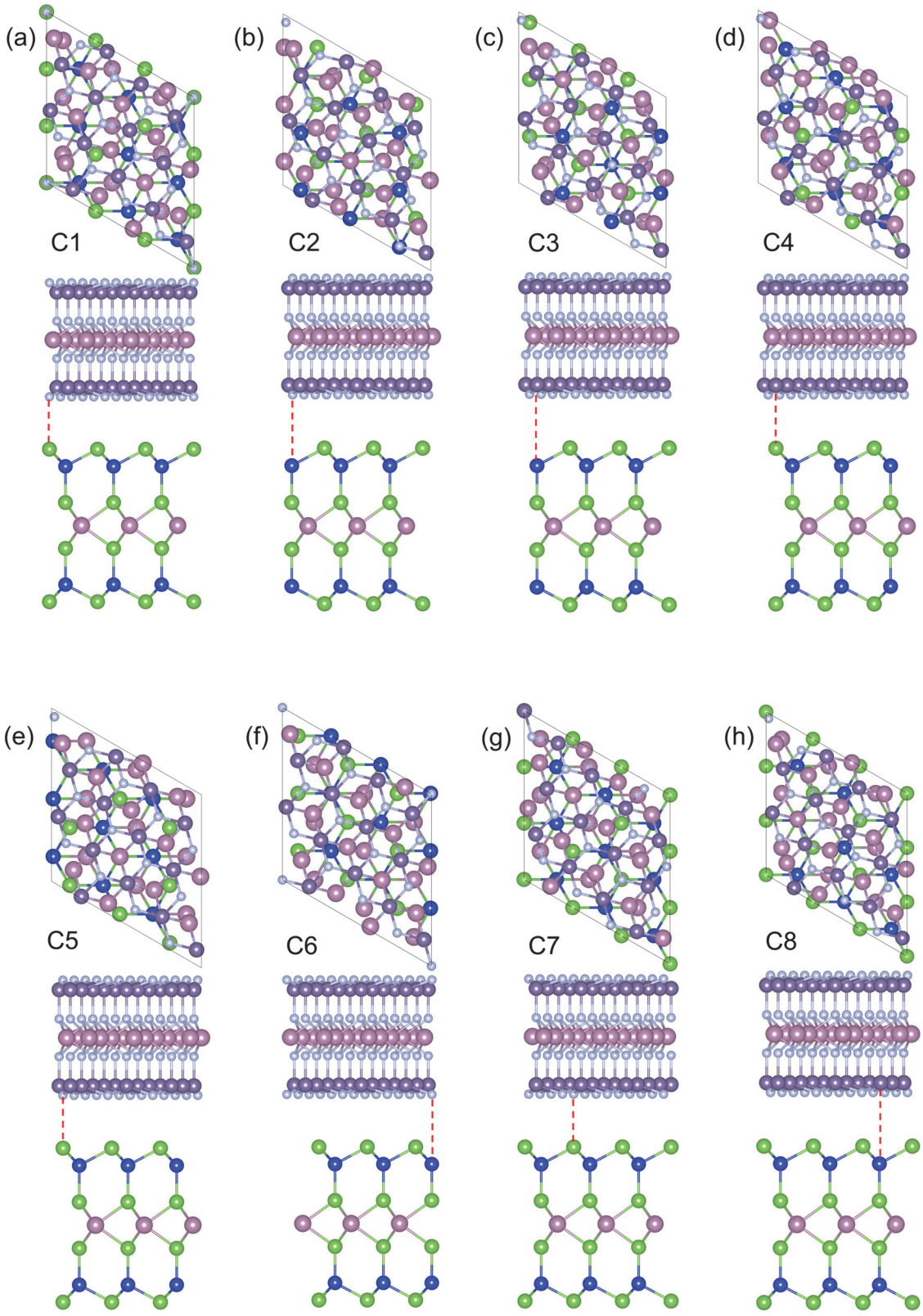

Fig. S3 Schematic atomic configurations of the $MoSi_2As_4/MoGe_2N_4$ vdW heterostructure, illustrating top and side views for eight distinct stacking configurations.

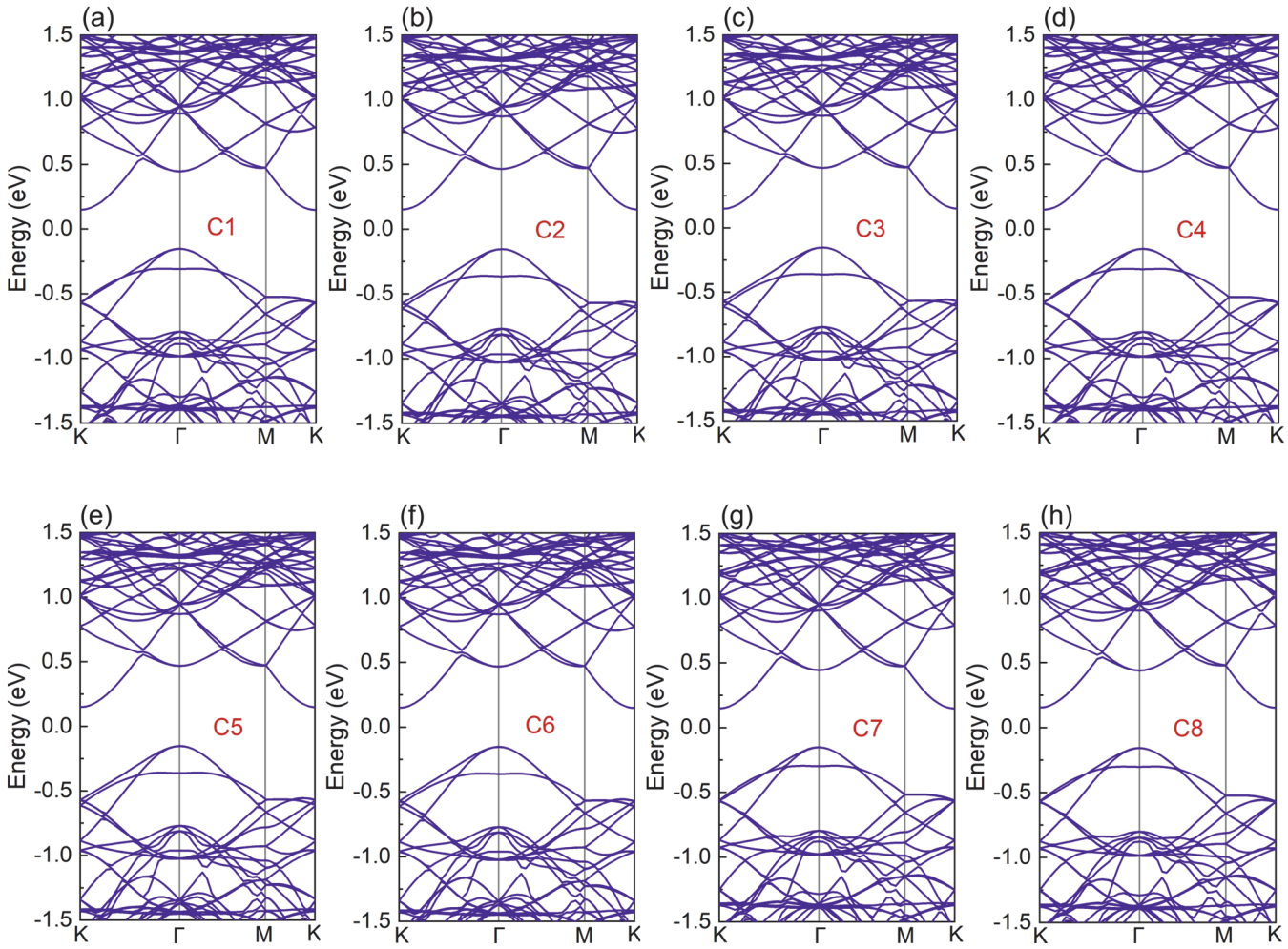

Fig. S4 Band structures (using PBE method) of eight distinct stacking configurations for $MoSi_2As_4/MoGe_2N_4$ vdW heterostructure.